Some Experimental and Theoretical Investigations on Fire Retardant Coir/Epoxy Micro-Composites

R. K. MISRA,[1,*] SANDEEP KUMAR,[2] K. SANDEEP,[3] ASHOK MISRA[1]

[1]*Department of Mechanical Engineering, B.I.T Mesra Ranchi, 835215, India*

[2]*Department of Polymer Engineering, Birla Institute of Technology Mesra, Ranchi, 835215*

[3]*Department of Mechanical Engineering, I.T., B.H.U. Varanasi-221005, India*

ABSTRACT: This article reports some experimental and theoretical investigations on fire retardant coir/epoxy micro-composites. The coir fiber is treated with saturated bromine water for increasing the electrical properties and then mixed with stannous chloride solution for improving the fire retardant properties. Only 5% (approximately) of fire retardant filler reduces the smoke density by 25% and the LOI value increases to 24%. The mechanical properties of the coir/epoxy micro-composites are not affected much after incorporation of filler. Flexural strength and flexural modulus of the NET increases tremendously compared to NEU and NE. Multiquadric radial basis function (MQRBF) method is applied for static and dynamic analysis of coir/epoxy micro-composite plate under uniformly distributed load. Damping behavior and natural frequencies are observed in NE, NEU, and NET. MQRBF is applied for spatial discretization and Newmark implicit scheme is used for temporal discretization. The discretization of the differential equations generates greater number of algebraic equations than the unknown coefficients. The multiple linear regression analysis, which is based on the least square error norm, is employed to obtain the coefficients. Simple supported and clamped boundary conditions are considered for verification of present results and they are compared with other existing analytical methods.

KEY WORDS: multiquadric radial basis function, coir fiber, fire retardant, epoxy resin.

*Author to whom correspondence should be addressed. E-mail: mishrark_kanpur@yahoo.com

0892-7057/07/00 0001–31 $10.00/0 DOI: 10.1177/0892705707084544

Los Angeles, London, New Delhi and Singapore

INTRODUCTION

NOWADAYS FIBER REINFORCED composites are considered important materials and have applications in aerospace, automobiles, defence, many more industries because of high strength and low-weight ratio. Therefore, there is need to have an efficient analytical method to analyze the behavior of fiber-reinforced composite structures. Finite element takes more time for generation of mesh therefore; new methods have been developed to handle these types of problems, which are known as meshless methods. These are element free Galerkin method [1], the reproducing kernel particle method [2], the smooth particles hydrodynamics [3], the partition of unity finite element [4], meshless Galerkin using radial basis functions [5], meshless local Petrov-Galerkin [6], modified smooth particle hydrodynamics [7] hp-clouds [8], the diffuse element [9], the natural element [10], Method of finite spheres [11] and wavelet Galerkin method [12]. Hardy [13] proposed the multiquadric radial basis function (MQRBF) for geographically scattered data interpolation. Later on, Kansa [14] used the MQRBF for solving the partial differential equations. Fedoseyev et al. [15] improved the accuracy of solution by placing the interior knots.

Combustion of materials depends on various parameters such as speed of flame, heat rate, fire endurance etc. If any of the above parameters can be modified in the material then these types of materials are called fire retardant material [16]. Epoxy resin constitutes the organic matrix for high performance composite material used in fabrication of light structured panels in the interior of an aircraft. The implication of these materials in fire propagation and flash over phenomena has led to reinforcement of the FFA regulations. New safety requirements limit the number of materials used in passenger areas. The choice of resin for an aircraft application requires heat and fire resistance [17]. Other application of fire retardant epoxy is printed circuit board. The principal component is the diglycidyl ether of tetrabrominated bisphenol A, which is mixed with antimony oxide for fire retardant properties [18].

Rose et al. [19] discussed about thermal oxidative degradation of an epoxy resin. They have proposed that the degradation leads to the formation of a surface carbonaceous material, which may take part in the protection of the resin. They have shown that the oxygen plays a part in the formation of a suitable carbonaceous material in the temperature range of 320–500°C and then in the degradation of the material in the temperature range 500–650°C. Toldy et al. [20] pointed out that phosphorylated hydroxyl phenols could be used as reactive flame-retardants for epoxy resin. Antimony trioxide and chlorine or bromine containing flame-retardants is classical in flame retardancy field. At the flame temperature this mixture

forms antimony trihalide vapor which scavenging hot radicals such as H-atom in the flame. Also, it forms blanket over the burn surface due to high density and removes oxygen from propagation front [21].

In the absence of halogenated compounds, Antimony oxide creates flame retardant effect in epoxy resin [22]. A major use for epoxy resins is in the manufacture of glass reinforced printed circuit boards. These often are composed of brominated epoxy resins based on tetrabromobisphenol A (TBBA). The purity of TBBA is critical in this application in order to reach more stringent electrical properties required by the electronics industry.

Antimony oxide is a stable system up to certain temperature. At flame temperature, it should react with halogen free radicals to form antimony halide. In this process, there is less possibility that 100% antimony oxide will be utilized. So to overcome this a matrix (coir) has been chosen, which can hold both halogen and antimony/tin, compounds covalently. Then this matrix is grinded to micro-dimensions and mixed with epoxy resin. After preparing coir/epoxy micro-composites Mechanical, optical and thermal properties are evaluated and results are presented in this article. In addition to this, MQRBF method is applied for static and dynamic analyses of the composite plate at uniformly distributed load.

EXPERIMENTAL STUDIES

Coir fibers contain 46% lignin and 43% cellulose [23]. For increasing the fire retardant properties of the coir fiber, it is treated with bromine water and mixed with stannous chloride. Due to presence of lignin, coir fibers can react easily with bromine water. After that, it is dried, grinded to micro-dimensions for better dispersibility, and mixed directly with epoxy resin.

Procedure for Epoxy-amine Composite Preparation

Epoxy resin (araldite) and hardener were procured from Huntsman Advanced Materials, Delaware, USA and coir fibers were obtained from local market. Stannous chloride of AR grade and liquid bromine were obtained from SD fine chemicals, Bombay, India.

Coir fiber was first segregated from spongy material and dewaxing of coir fiber was done as per the procedure followed by Khalid et al. [24]. According to this procedure, the coir fiber was extracted in a soxhlet apparatus with a mixture of 4:1:1 (by weight) toluene, methylated spirit and acetone for 4–5 h. The extracted fiber was kept overnight in an oven at $105 \pm 5^{\circ}C$ for drying.

The dewaxed coir fiber was brominated with saturated bromine water for increasing the electrical properties and approximately 10 gm of dewaxed coir fiber was dipped into 300 ml of saturated bromine water for 48 h. It was removed and washed thoroughly with distilled water for several times and then dried in oven at $105 \pm 5^{\circ}C$.

The brominated coir fiber was mixed with stannous chloride solution. Due to presence of tin, fire retardant properties of the coir fibers increased. After mixing with stannous chloride solution, coir fiber was boiled until it was evaporated to dryness. Then the mixture was dried in oven at $105 \pm 5^{\circ}C$. In this drying process, coir fiber became black. This black fiber was grinded to powder and particle size was measured.

Liquid epoxy resin (Araldite) and hardener (amine) in 1:0.8 ratio was taken in a plastic container and mixed thoroughly for 15 min. Then it was poured into a plastic mould for 24 h. After that pellet was removed from mould and heated at $105 \pm 5^{\circ}C$ in an oven for 3 h. For composite preparation, epoxy resin was taken in plastic container and the coir fiber was added to it. Then it was mixed thoroughly before addition of hardener and poured into a plastic mould.

Characterization of Coir Fiber

FOURIER TRANSFORM INFRA RED(FTIR) SPECTRA

(FTIR) spectra of coir fiber of dewaxed, brominated and micro-powder was done by Schemazdu IR prestige 21 models by diffuse reflectance spectroscopy technique. The spectral behavior of dewaxed coir fiber and brominated coir fiber were almost same except for the decrease in peak intensity at almost all positions. The peak near $3600\,cm^{-1}$ may be due to the free phenolic -OH group, which reduces after bromination. In addition, the carbonyl group intensity near $1720\,cm^{-1}$ reduced after bromination. The decrease in the two-peak intensity showed that bromination had taken place.

DIFFERENTIAL SCANNING CALORIMETRY (DSC)

The dewaxed coir fiber showed an endothermic peak near 90°C and an exothermic peak started after 220°C. The endothermic peak was mostly due to the adsorbed moisture content and exothermic peak due to the degradation of the coir fiber. On the other hand, brominated coir fiber showed a wide range endothermic peak, which started below room temperature to 200°C and the peak position near 117°C. This may be due to the removal of moisture from the sample. Another endothermic peak was observed after 248°C. This proved that the bromination had taken place.

Evaluation of Fibers Properties

The denier and tex of fibers were determined by measuring the weight of fibers of known length. An average of five samples were taken. The diameter of the fibers was calculated from density and denier of the fibers.

Mechanical properties of fibers were evaluated using a Zwick tensile testing machine (model Z010). For each sample, 30 fibers were tested at the following specifications-gauge length = 50 mm, crosshead speed = 10 mm/min. Fibers with constant gauge length were clamped in the jaws mounted on the tensile testing machine and stressed under uniaxial tension. The initial modulus, tenacity, and elongation at break were calculated from the resulting stress-strain curves.

Light Scattering

The micro-coir powder was taken in Malvern Nano ZS model in aqueous suspension for the study of particle size of the fire retardant coir/epoxy micro-composites, using light scattering technique.

Smoke Density

Smoke can be defined as a dispersion of solid or liquid particles in a carrier gas and generally has relatively little toxicity associated with it if the carrier gas is nontoxic. It is believed that more of the deaths in fire occur due to smoke rather than direct burning, since it obscures the visibility and seriously impairs the ability of a person to escape the fire hazard. Hence smoke suppression or alternatively light transmittance is very important. Smoke generation can be measured as the percent obscuration by burning of the sample of dimensions $2.54 \times 2.54 \times 0.6\,cm^3$. The test was carried out in a Platon smoke density chamber from S.A. Associates, New Delhi designed to meet ASTM D-2483 flammability test requirement.

The sample was kept on a wire – net and ignited by a flame of 40-psi pressure keeping the burner at an angle of 45°. Smoke generation was measured as obscuration posed by smoke to a light source. For this purpose, a bulb of 5.80 W was used in the chamber. Obscuration was noted after every 15 s with an alarm sound. Sixteen readings were noted and each test took 4 min for completion.

Limiting Oxygen Index (LOI)

LOI is the minimum percentage of oxygen in an atmosphere of oxygen-nitrogen mixture (by volume), which is required to sustain candle like

burning of the specimen for 3 min and was calculated using the following formula,

$$\mathrm{LOI} = \frac{\text{oxygen}}{(\text{oxygen} + \text{nitrogen})} \times 100$$

The dimension of the samples was $100 \times 6 \times 0.6$ mm. In this test, specimen was clamped at the bottom in a closed chamber. The sample was ignited at the upper and with a constant hydrogen flame. The flow rate of the mixture of gases was at 10.6 L/min. Electronic digital meter connected with the instrument showed the percentage of oxygen in the mixture. Five samples were tested for each sample and an average value was reported.

Mechanical Properties

Properties of the coir and modified coir fibers have been shown in Table 1. After grinding coir fiber, passed through 70-mesh sieve sizer according to ASTM D. Particle size analyzer measured the size of coir fibers; it was in the range of approximately 800–900 nm.The specimen had dimensions, $50 \times 7.1 \times 1.75$ mm according to ASTM D638. Compositions of the specimens are given in Table 2.

Table 3 shows the tensile properties of pure epoxy, untreated coir fiber reinforced epoxy and treated coir fiber reinforced epoxy composites. The tensile strength and elongation at break of the Net Epoxy (NE) resin are higher than those Net Epoxy Untreated (NEU) micro-coirs reinforced

Table 1. Properties of the coir and modified coir fibers.

Properties	Unmodified coir	Brominated Coir
Diameter (μm)	20.2	22.3
Denier (g)	10.8	12.5
Tensile Strength (g/denier)	2.6	3.2
Tensile Modulus (g/denier)	224.6	201.2
Elongation at break (%)	1.6	1.1

Table 2. Compositions of the coir fiber reinforced composites.

Sample designation	Epoxy (g)	Hardener (g)	Fiber (g)
NE	20	14	0
NEU	20	14	1.6 (untreated)
NET	20	14	1.6 (treated)

epoxy composites and Net Epoxy Treated (NET) micro-coirs reinforced epoxy composites. However, the tensile modulus of the NEU and NET samples increases by 19% and 15%, respectively than NE sample. Surface modification could effectively enhance the fiber matrix bond strength.

Table 4 presents the flexural properties of the composites. In all the cases, the flexural strength and flexural modulus of the composite materials (NEU and NET) are higher than unfilled epoxy matrix (NE). There is 38% of increase in flexural strength in treated fiber composites (NET) samples compared to neat matrix (NE) samples, whereas there is 111% of increase in the flexural modulus of treated fiber composites compared to neat matrix. This is natural for composite material. Epoxy resin is a brittle plastic. Its impact properties can be improved by incorporation of rubbery or any other hetero phase such as filler material but this decreases the mechanical properties like tensile strength and elongation. On the other hand, it may improve the flexibility, which is observed in this case.

Fire Retardant Properties

Table 5 shows the fire retardant properties of the composites. Two fire retardant properties, viz., smoke density and LOI, were analyzed. Pure epoxy composites have more smoke density percentage compared to micro-filler epoxy amine composites. Analyses show that the fire retardant properties of the composites increase due to epoxy resin. Smoke density of NEU is more than that of NE because coir fibers were

Table 3. Tensile properties of the composites.

Sample Designation	Tensile strength (MPa)	Tensile Modulus (MPa)	Elongation at break (%)
NE	23.00	0.6984	11.10
NEU	20.21	0.8333	6.98
NET	19.48	0.8056	7.65

Table 4. Flexural properties of the composites.

Sample Designation	Flexural strength (MPa)	Flexural Modulus (MPa)
NE	51.62	1485
NEU	53.83	1881
NET	71.20	3140

Table 5. Fire retardant properties of the composites.

Sample Designation	Smoke Density (%)	LOI (%)
NE	46.78	31.50
NEU	49.65	35.64
NET	34.42	38.90

treated with bromine. The percentage of LOI of NET is higher compared to those of NEU and NE.

After evaluating the mechanical and thermal properties of the coir/epoxy micro-composites, MQRBF method is applied for static and dynamic analyses of the coir/epoxy micro-composite plate to assess its response to external loading such as uniformly distributed load.

THEORETICAL INVESTIGATIONS

The Multiquadric Radial Basis Function Method

Consider $P_1, P_2, P_3, P_4, \ldots, P_N$ being N collocation points in domain Ω of which $P_i(i = 1, 2, 3, \ldots, N_I)$ are interior points and $P_i(i = N_{I+1}, \ldots, N)$ are boundary points. Partial differential equation for boundary value problems has been given below:

$$Aw = f(x, y) \quad \Omega \, , C \, , \mathbf{R}^n \tag{1}$$

$$Bw|_{\partial\Omega} = g(x, y) \quad \in R^n \tag{2}$$

A is linear differential operator, B is a linear boundary operator imposed on boundary conditions. In Eigen value problems, the Equations (1) and (2) reduce to

$$Aw = \lambda^4 w \tag{3}$$

$$Bw = 0 \tag{4}$$

Solution of Equations (1) and (2) is expressed as:

$$w(x, y) = \sum_{j=1}^{N} w_j \varphi_j(x, y) \tag{5}$$

$\{w_j\}_{j=1}^{N}$ are the unknown coefficients to be determined, and $\varphi_j(x_j, y_j)$ is a basis function.

$$\varphi_j = \sqrt{(x - x_j)^2 + (y - y_j)^2 + c^2} = \sqrt{r_j^2 + c^2} \tag{6}$$

Other widely used radial basis functions are:

$\varphi(r) = r^3$	Cubic
$\varphi(r) = r^2 \log(r)$	Thin plate splines
$\varphi(r) = (1 - r)_+^m p(r)$	Wendland functions
$\varphi(r) = e^{-(cr)^2}$	Gaussian
$\varphi(r) = (c^2 + r^2)^{-1/2}$	Inverse multiquadrics

Here $r = ||P - P_j||$ is the Euclidean norm between points $P = (x, y)$ and $P_j = (x_j, y_j)$. The Euclidian distance r is real and nonnegative and c is a shape parameter, a positive constant. Ling and Kansa [25] discussed in details about the shape parameter.

Calculation of Eigen Values

Let N_B be the total points on the boundary $\partial\Omega$, N_I be the total points inside Ω and $N = N_I + N_B$. Applying the RBF in Equation (3),

$$\sum_{j=1}^{N} w_j A\varphi\left\|P_i - P_j\right\| = \lambda^4 \sum_{j=1}^{N} w_j \varphi\left\|P_i - P_j\right\| \tag{7}$$

where $i = 1, 2, \ldots, N_I$
Define

$$\mathbf{L} = [A\phi(\left\|P_i - P_j\right\|)]_{N_I \times N} \tag{8}$$

$$\mathbf{M} = \left[\phi||P_i - P_j||\right]_{N_I \times N} \tag{9}$$

Applying MQRBF in Equation (4),

$$\sum_{j=1}^{N} w_j B\phi(\left\|P_i - P_j\right\|) = 0 \tag{10}$$

where $i = N_{I+1}, N_{I+2}, \ldots, N$

$$\mathbf{K} = \left[B\phi(\left\|P_i - P_j\right\|)\right]_{N_B \times N} \tag{11}$$

$$\mathbf{w} = [w_1\ w_2\ w_3 \ldots w_N]^T \tag{12}$$

Equations (7) and (12) can be written as:

$$\mathbf{Lw} = \lambda^4 \mathbf{Mw} \tag{13}$$

$$\mathbf{Kw} = 0 \tag{14}$$

General eigen value problem in the matrix form becomes

$$\begin{bmatrix} \mathbf{L} \\ \mathbf{K} \end{bmatrix} \mathbf{w} = \lambda^4 \begin{bmatrix} \mathbf{M} \\ 0 \end{bmatrix} \mathbf{w} \tag{15}$$

The following algorithm [26] of the standard eigen value problem has been used in the present analysis.

$$\mathbf{L}^1 \mathbf{w}^2 = \lambda^4 \mathbf{w}^2 \tag{16}$$

where:

$$\mathbf{L}^1 = \mathbf{L}\mathbf{D}^{-1} \begin{bmatrix} \mathbf{I}_{N_I x N_I} \\ \mathbf{0}_{N_B x N_I} \end{bmatrix} \tag{17}$$

$$\mathbf{w}^2 = [w_1 \; w_2 \; w_3 \ldots w_N]^T \tag{18}$$

$$\mathbf{D} = \begin{bmatrix} \mathbf{M} \\ \mathbf{K} \end{bmatrix} \tag{19}$$

RESULTS AND DISCUSSION

Coir fibers possess substantial amount of cellulose (~43%) and lignin (~46%) having a network type of structure with majority of methoxy and free hydroxyl groups. Bromine water can react from both types of materials. Phenol can easily react with bromine water and give tribromo phenol. Bromine water can oxidize the aldehyde group to acid. No literature is available on the surface modification of coir fiber by bromine water. Coir fibers show lot of porosity from the Scanning Electron Microscope (SEM). Since lot of porosity is present on the coir surface, so bromine can easily enter into the pores and react with the inner layer.

Diameter of the coir fiber is increased after bromination; this may be due to the addition of bromine, which is heavier and bigger in size in the molecular structure. This supports the increase in denier value after bromination. In this process, tensile strength is increased where as tensile modulus and percentage elongation at break is decreased. That means the fiber is easily breakable after bromination. After treated with bromine and stannous chloride solution, fire retardant performance of the coir fiber is improved.

NET sample shows less change in thermal behavior than pure epoxy composites. Poisson ratio of the NET sample is 0.3 and tensile Modulus $E_R = 0.8056$ MPa (Table 3).

Case Study 1: Static and Dynamic Response of the of Composite plate

Figure 1 shows the geometry, coordinate system and loading in coir/epoxy micro-composites plate. Neglecting the transverse shear and rotary inertia, governing equation of the plate is expressed in nondimensional form as:

$$(w_{xxxx} + 2R^2 w_{xxyy} + R^4 w_{yyyy}) + w_{tt} + c_v w_t - Q(x, y, t) = 0 \qquad (20)$$

$$w = \frac{w^*}{h}, x = \frac{x^*}{a}, y = \frac{y^*}{b}, R = \frac{a}{b}, t = t^* \sqrt{\frac{D}{(\rho a^4 h)}}$$

$$Q = \frac{qa^4}{(Dh)}, D = \frac{Eh^3}{12(1-\nu^2)}, C_v = \frac{C_v^*}{m} \sqrt{\frac{(\rho a^4 h)}{D}}, m = \rho abh,$$

Simply supported boundary conditions for all four edges are:

$$x = 0, a \quad w = 0 \qquad (21a)$$

$$x = 0, a \quad w_{xx} = 0 \qquad (21b)$$

$$y = 0, b \quad w = 0 \qquad (21c)$$

$$y = 0, b \quad w_{xx} = 0 \qquad (21d)$$

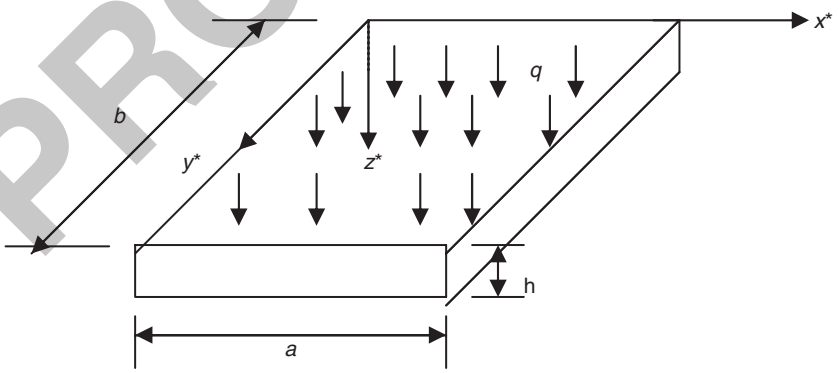

Figure 1. *Geometry of the coir/epoxy micro composites plate.*

Clamped boundary conditions for all four edges are:

$$x = 0, a \quad w = 0 \tag{22a}$$
$$x = 0, a \quad w_x = 0 \tag{22b}$$
$$y = 0, b \quad w = 0 \tag{22c}$$
$$y = 0, b \quad w_x = 0 \tag{22d}$$

MQRBF method is applied in the governing Equations (20) and boundary conditions (Equation 21 or Equation 22), and presented in Appendix A. It generates more algebraic equations than the unknown coefficients. To solve this incompatibility, the multiple linear regression analysis (Appendix B) based on least-square error norms is employed.

Deflection of the coir/epoxy micro-composites plate at various aspect ratios of the present method for simply supported and clamped edge boundary conditions have been compared with those obtained by Timoshenko and Woinowsky-Krieger [27] as shown in Tables 6 and 7, respectively. There is good agreement between the present results and reference solution for both simply supported and clamped edge boundary conditions.

Table 6. Deflection of simple supported coir/epoxy micro-composite plate with variation of aspect ratio.

q (N/m^2)	b (mm)	a (mm)	b/a	h (mm)	Analytical Method w_{max} [27] (mm)	Radial basis Method w_{max} (mm)
10	300	300	1.0	10	4.4561	4.5000
10	300	150	2.0	10	0.6949	0.6928
10	300	100	3.0	10	0.1657	0.1653
10	300	50	6.0	10	0.0110	0.0110

Table 7. Deflection of clamped edge coir/epoxy micro-composite plate with variation of aspect ratio.

q (N/m^2)	b (mm)	a (mm)	b/a	h (mm)	Analytical Method w_{max} [27] (mm)	Radial basis Method w_{max} (mm)
10	300	300	1.0	10	1.3829	1.3171
10	300	200	1.5	10	0.4770	0.4553
10	300	150	2.0	10	0.1742	0.1715
10	300	50	6.0	10	0.0022	0.0022

Figures 2 and 3 show deflection at various aspect ratios and uniformly distributed load 10 N/m^2, at simple supported and clamped edge boundary conditions, respectively. In case of simple supported boundary conditions, variation in deflection is less after aspect ratio 3 and in clamped edge boundary conditions, variation in deflection is less after aspect ratio 2 as shown in Figures 2 and 3, respectively.

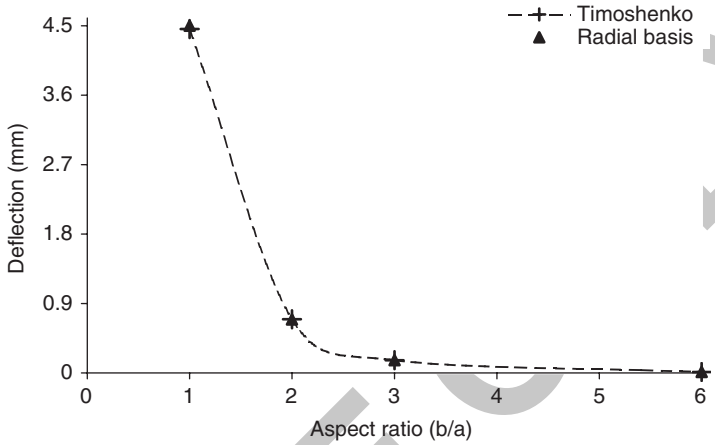

Figure 2. *Deflection of simple supported coir/epoxy micro-composite plate at various aspect ratios.*

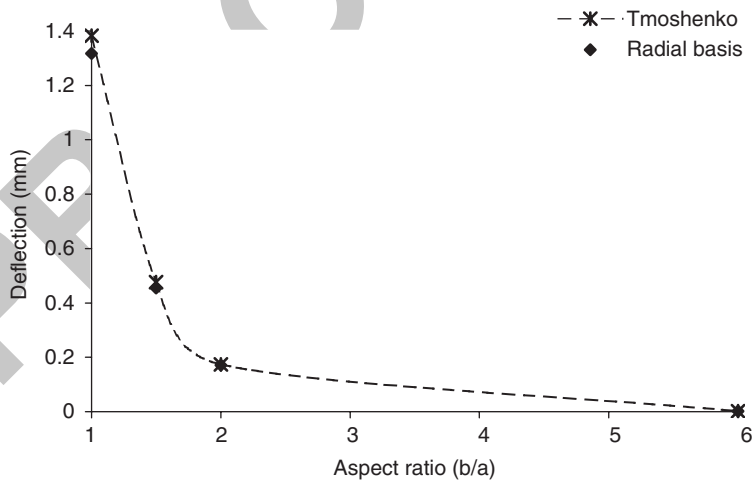

Figure 3. *Deflection of clamped edge coir/epoxy micro-composite plate at various aspect ratios.*

Dynamic analysis of epoxy resin, untreated coir fiber reinforced composite and treated coir fiber reinforced composite plate are performed by MQRBF. The damped response of present and finite difference methods have been compared and shown in Figures 4 and 9. Figure 4 shows the damped response of a simple supported epoxy resin square plate and Figure 9 shows the damped response of a simple supported treated coir fibers reinforced epoxy resin composite plate at damping coefficient factor $C_v = 1.25$. In both case there is good agreement in results.

Damped dynamic response of epoxy resin, untreated coir fiber reinforced composite and treated coir fiber reinforced composite plate at various damping factor and aspect ratio has been performed which has been shown in Figures 5–11. According to present method, at aspect ratio $b/a = 1$, maximum deflection in epoxy resin square plate is 0.6737, 0.6757, and 0.672, in untreated coir fiber reinforced composite plate is 0.5651, 0.5668, and 0.5637 and treated coir fiber reinforced composite plate is 0.5843, 0.586, and 0.5828, respectively at damping factor $C_v = 1.25$, 6, and 10 as shown in Figures 5, 7, and 10. However, the fluctuation in deflection with $C_v = 6.0$ and 10, die out rapidly after the nondimensional time 12 at $C_v = 6.0$ and 9.6, 9.9 and 9.6 at $C_v = 10$ in epoxy resin, untreated coir fiber reinforced composite and treated coir fiber reinforced composite plate, respectively.

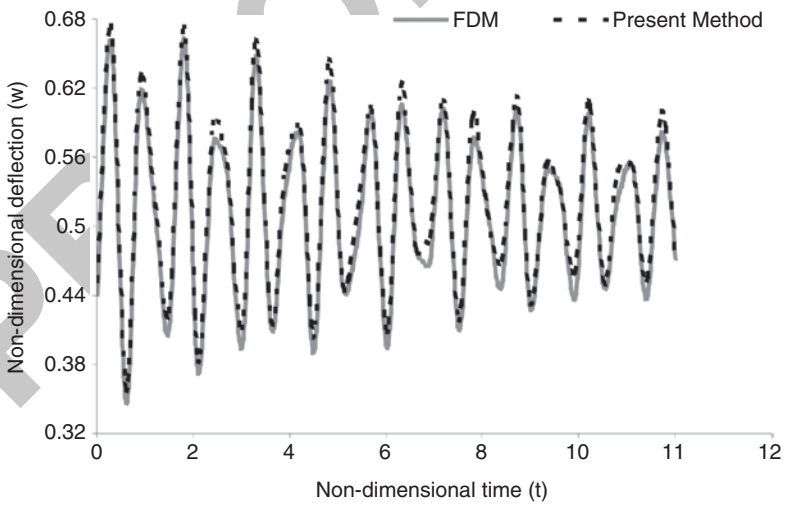

Figure 4. *Damped response of a simple supported epoxy resin square plate at damping coefficient factor, $C_v = 1.25$.*

Further, at aspect ratio $b/a = 2$, maximum deflection in epoxy resin is 0.099, 0.0937, and 0.0888, in untreated coir fiber reinforced composite, is 0.083, 0.0786, and 0.0745 and in treated coir fiber reinforced composite plate is 0.0859, 0.0812, 0.077 at $C_v = 1.25$,6, and 10 as shown in Figures 6, 8 and 11.

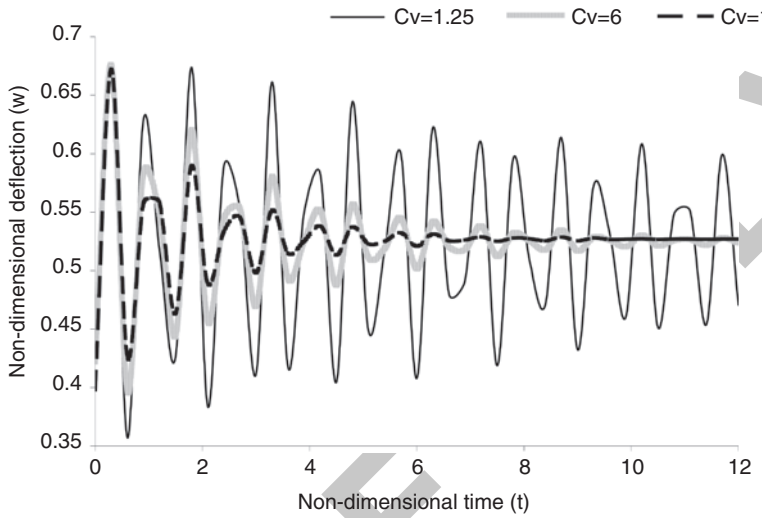

Figure 5. *Damped response of a simple supported epoxy resin isotropic plate for aspect ratio, b/a = 1.*

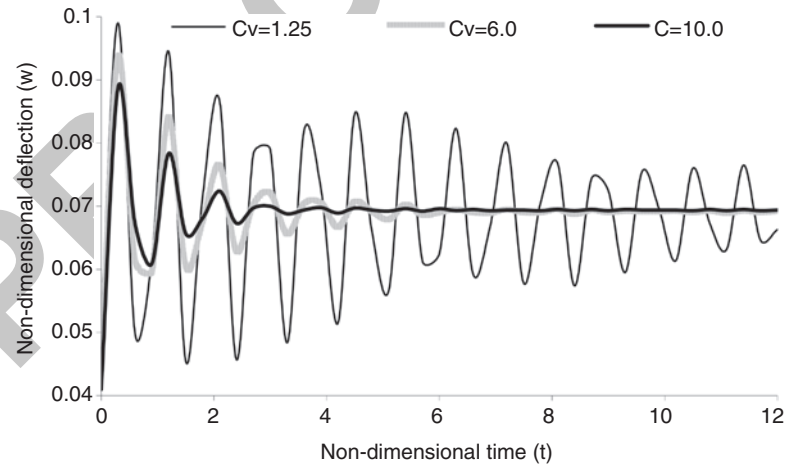

Figure 6. *Damped response of a simple supported epoxy resin isotropic plate for aspect ratio, b/a = 2.*

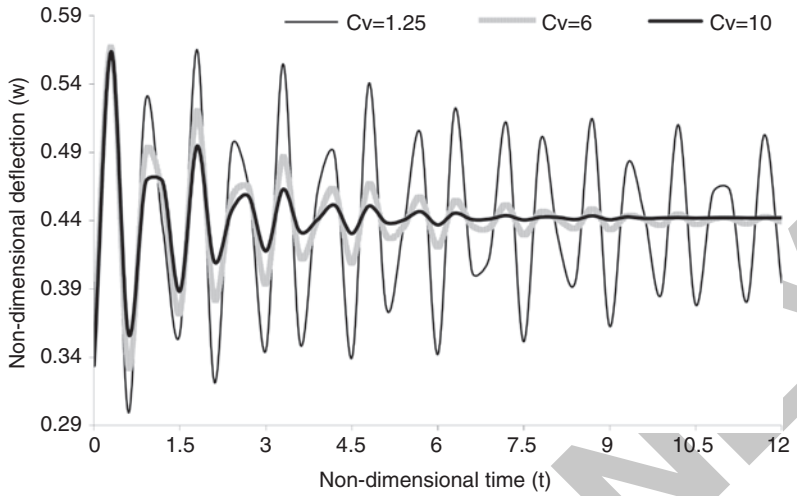

Figure 7. *Damped response of a simple supported untreated coir fibers reinforced epoxy resin composite plate for aspect ratio, b/a = 1.*

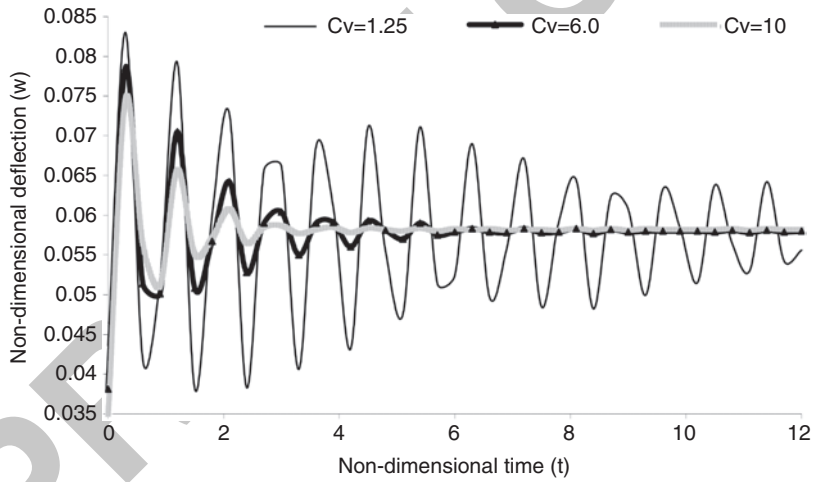

Figure 8. *Damped response of a simple supported untreated coir fibers reinforced epoxy resin composite plate for aspect ratio, b/a = 2.*

However, the fluctuation in deflection with $C_v = 6.0$ and 10, die out rapidly after the nondimensional time 9, 4.8 in epoxy resin square plate, 9.3, 5.1 in untreated coir fiber reinforced composite plate and 9, 4.8 treated coir fiber reinforced composite plate, respectively.

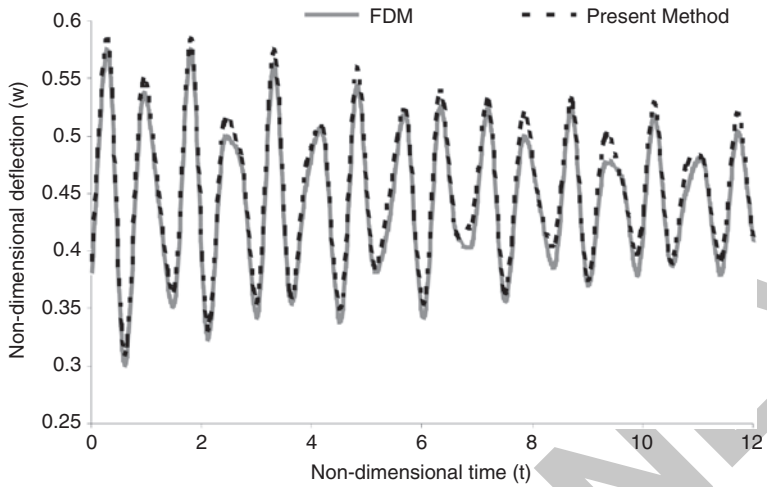

Figure 9. *Damped response of a simple supported treated coir fibers reinforced epoxy resin composite plate at damping coefficient factor, $C_v = 1.25$.*

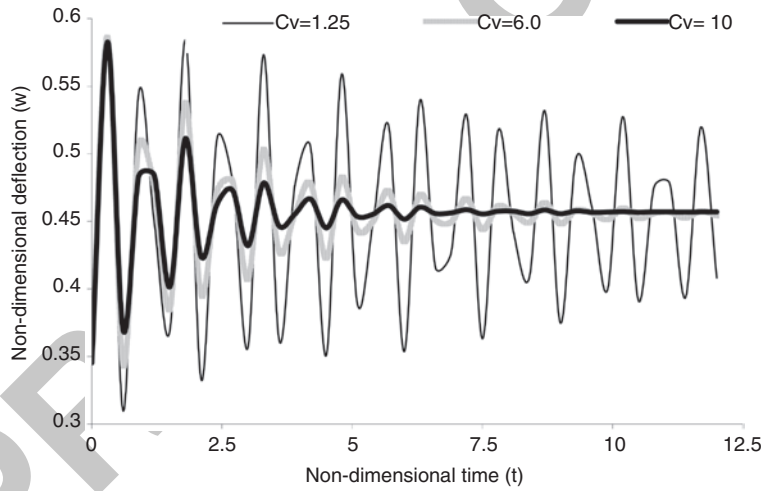

Figure 10. *Damped response of a simple supported treated coir fibers reinforced epoxy resin composite plate for aspect ratio, $b/a = 1$.*

Following features are observed after analyzing the Figures 5–8, 10 and 11 and Tables 8 and 9 in simple supported boundary conditions:

- Maximum deflection amplitude is highest in epoxy resin square plate and least in untreated coir fiber reinforced composite plate. It means strength

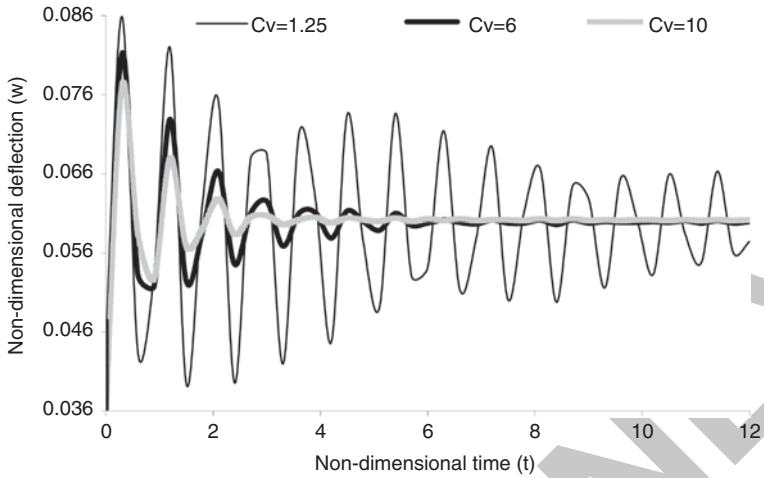

Figure 11. *Damped response of a simple supported treated coir fibers reinforced epoxy resin composite plate for aspect ratio, b/a = 2.*

Table 8. Dynamic behavior of simple supported epoxy resin, treated and untreated coir/epoxy micro composite plates at aspect ratio b/a = 1.

Materials	Non dimensional maximum amplitude	Non dimensional Time to stabilize
$C_v = 1.25$		
NE	0.673	Did not stabilize even after 12
NET	0.5843	
NEU	0.5651	
$C_v = 6$		
NE	0.6757	Stabilize after 12
NET	0.586	
NEU	0.5668	
$C_v = 10$		
NE	0.672	Stabilize after 9.6
NET	0.5828	Stabilize after 9.6
NEU	0.5637	Stabilize after 9.9

of the untreated coir fiber reinforced composite plate are higher as compared to treated coir fiber reinforced composite plate and epoxy resin square plate. It is clear from Table 3 that tensile modulus is highest in untreated coir fiber reinforced composite plate and least in epoxy resin square plate.

- As damping coefficient increases, stability time decreases.

Table 9. Dynamic behavior of simple supported epoxy resin, treated and untreated coir/epoxy micro composite plates at aspect ratio b/a = 2.

Materials	Non dimensional maximum amplitude	Non dimensional Time to stabilize
$C_v = 1.25$		
NE	0.099	Did not stabilize even after 12
NET	0.0859	
NEU	0.083	
$C_v = 6$		
NE	0.0937	Stabilize after 9
NET	0.0812	Stabilize after 9
	0.0786	Stabilize after 9.3
$C_v = 10$		
NE	0.0888	Stabilize after 4.8
NET	0.077	Stabilize after 4.8
NEU	0.0745	Stabilize after 5.1

- Pure epoxy resin square plate stabilizes fast as compared to untreated coir fiber reinforced composite plate.
- Pure epoxy resin square plate and treated coir fiber reinforced composite plate stabilize at same time.
- When aspect ratio increases, stability time and maximum nondimensional deflection amplitude decrease. In this case, as aspect ratio increases, area decreases which has been shown in Tables 6 and 7. Here width, b is constant and only length a decreases. As area decreases total load on plate decreases. Due to decrease in load, deflection also decreases.

It may be noted here that pure epoxy resin square plate stabilizes fast as compared to untreated coir fiber reinforced composite plate. Actually, after reinforcing the fiber, damping property of the composite plate decreases and stiffness improves. Other reason could be elastic nature of the fiber. When interfacial bonding improves, damping property decreases. Therefore, deflection is less in untreated coir fiber reinforced composite plate and stabilizes slow as compared to pure epoxy resin.

As evident from Tables 8 and 9 pure epoxy resin square plate and treated coir fiber reinforced composite plate stabilize at the same time. Coir fibers show lot of porosity under SEM. Since lot of porosity is present on the coir surface, so bromine can easily enter into the pores and react with the inner layer. Diameter of the coir fiber increases after bromination. Damping property of the treated coir fiber reinforced composite plate increases because coir fibers become brittle due to the treatment from bromine. This improves the stability of the composite plate.

Similarly, Figures 12–17 and Tables 10 and 11 show the damped response of pure epoxy resin square plate, untreated coir fiber reinforced composite plate and treated coir fiber reinforced composite plate at clamped edge boundary conditions. But in clamped edge boundary condition, deflection of the plate is less and stabilizes late as compared to simple supported boundary condition.

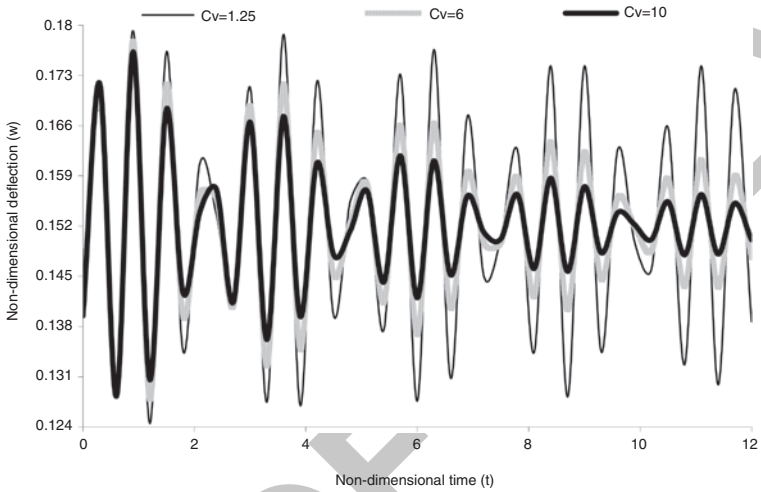

Figure 12. *Damped response of a clamped edge epoxy resin isotropic plate for aspect ratio,*

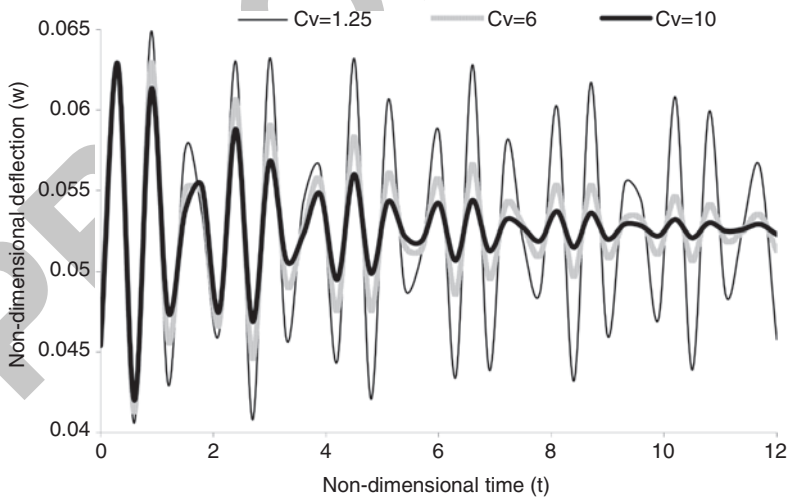

Figure 13. *Damped response of a clamped edge epoxy resin isotropic plate for aspect ratio, b/a = 1.5.*

Case Study 2: Governing Differential Equations for Free Vibration of Coir/Epoxy Micro Composite Plate

Coir/epoxy micro-composite plate behaves similar to isotropic plate. Elasticity is same in all the direction in this composite plate; therefore governing differential equation is same. The governing differential equation for a free flexural vibration of a uniform thin isotropic plate in

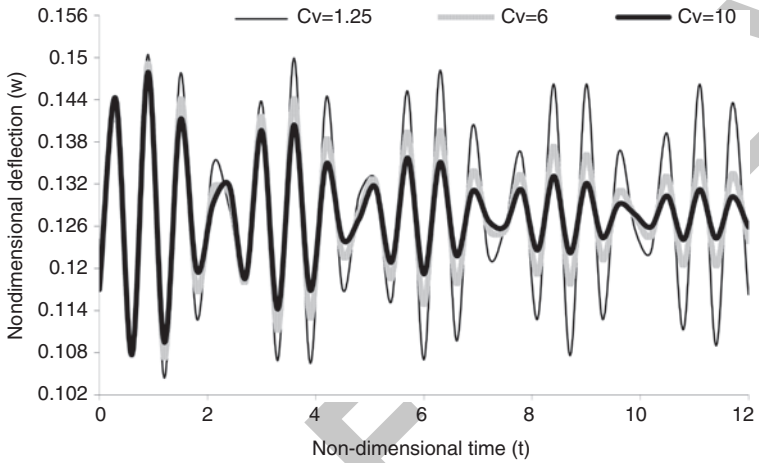

Figure 14. *Damped response of a clamped edge untreated coir fibers reinforced epoxy resin composite plate for aspect ratio, b/a = 1.*

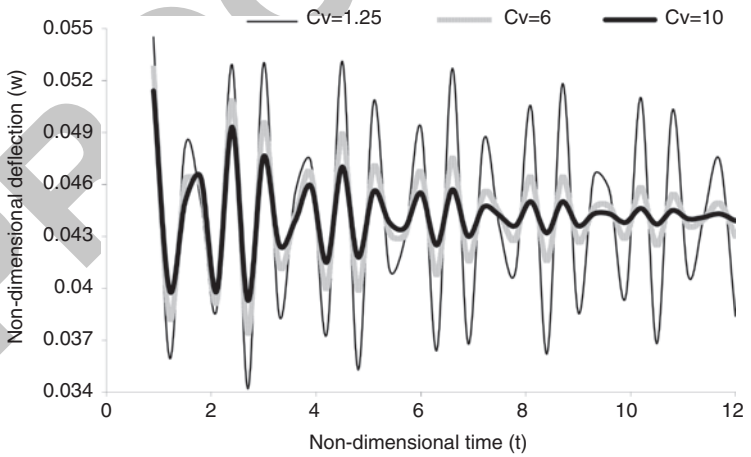

Figure 15. *Damped response of a clamped edge untreated coir fibers reinforced epoxy resin composite plate for aspect ratio, b/a = 1.5.*

nondimensional form is written as follows [28]:

$$\frac{1}{a^4}\left(\frac{\partial^4}{\partial x^4}+2R^2\frac{\partial^4}{\partial x^2\partial y^2}+R^4\frac{\partial^4}{\partial y^4}\right)w=\lambda^4 w(x,y) \tag{23}$$

$$\lambda^4=\frac{\omega^2\rho_0 h}{D} \tag{24}$$

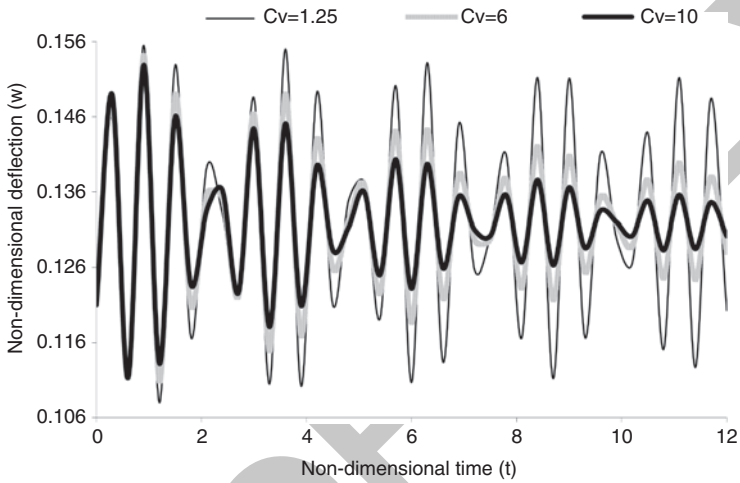

Figure 16. *Damped response of a clamped edge treated coir fibers reinforced epoxy resin composite plate for aspect ratio, b/a = 1.*

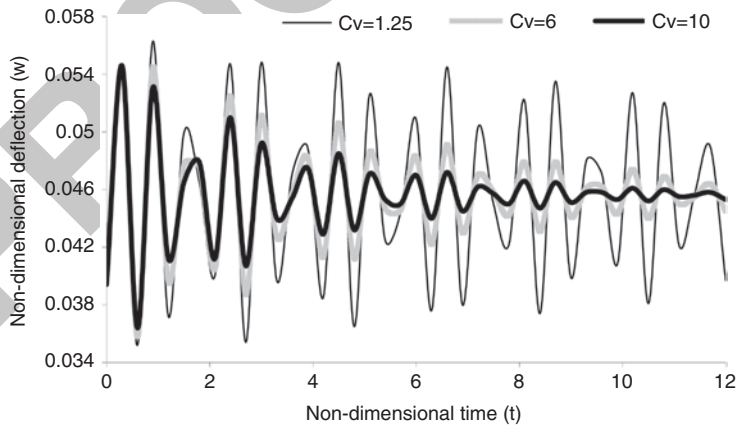

Figure 17. *Damped response of a clamped edge treated coir fibers reinforced epoxy resin composite plate for aspect ratio, b/a = 1.5.*

where w is displacement, ρ_0 is surface density, λ and ω are eigen values and natural frequency respectively. The flexural rigidity $D = Eh^3/12(1-\nu^2)$, where E is Young's modulus of the coir/epoxy micro-composite plate, ν is Poisson ratio and h is the plate thickness. The natural frequency of simply supported isotropic plate is obtained by Ashton and Whitney [29] as

$$\omega_{mn} = \frac{\pi^2}{R^2 b^2}\sqrt{\frac{D}{\rho_0}}\sqrt{m^4 + 2m^2n^2R^2 + n^4R^4} \tag{25}$$

Table 10. Dynamic behavior of clamped edge epoxy resin, treated and untreated coir/epoxy micro composite plates at aspect ratio b/a = 1.

Materials	Non dimensional maximum amplitude
$C_v = 1.25$	
NE	0.1793
NET	0.1555
NEU	0.1504
$C_v = 6$	
NE	0.1777
NET	0.1541
NEU	0.1491
$C_v = 10$	
NE	0.1763
NET	0.1529
NEU	0.1479

Table 11. Dynamic behavior of clamped edge epoxy resin, treated and untreated coir/epoxy micro composite plates at aspect ratio b/a = 1.5.

Materials	Non dimensional maximum amplitude
$C_v = 1.25$	
NE	0.0649
NET	0.0563
NEU	0.0545
$C_v = 6$	
NE	0.0629
NET	0.0545
NEU	0.0527
$C_v = 10$	
NE	0.0629
NET	0.0546
NEU	0.0514

where m and n are integers. Different natural frequencies are obtained at different combinations of m and n. On the other hand, Hearmon [30] has expressed the natural frequencies of clamped supported plate as:

$$\omega_{mn} = \frac{1}{a^2}\sqrt{\frac{D}{\rho_0}}\sqrt{\alpha_1^4 + 2\alpha_2 R^2 + \alpha_3^4 R^4} \tag{26}$$

where α_1, α_2, and α_3 are the coefficients and their values have been given in Table 12.

Substituting the property values of epoxy resin, untreated coir fiber reinforced composites and treated coir fiber reinforced composites in Equations 25 and 26 the natural frequencies of free vibration at simple supported and clamped edge boundary conditions have been evaluated by the present method and by Ashton & Whitney [29] and Hearmon [30] methods. Following observation are made from Tables 13–15.

- There is good agreement in results obtained by Ashton & Whitney (1970) and present methods.
- Values of natural frequencies are higher in untreated coir fibers reinforced epoxy resin square composite plate as compared to treated coir fibers reinforced epoxy resin square composite plate and epoxy resin

Table 12. Coefficients for natural frequency calculations.

Boundary Conditions	α_1	α_3	α_2	m	n
All edges are clamped	4.730	4.730	151.3	1	1
	4.730	$(n+0.5)\times 3.14$	$12.30\alpha_3\ (\alpha_3 - 2)$	1	2,3,4
	$(m+0.5)\times 3.14$	4.730	$12.30\alpha_1\ (\alpha_1 - 2)$	2,3,4	1
	$(m+0.5)\times 3.14$	$(n+0.5)\times 3.14$	$\alpha_1\alpha_3\ (\alpha_1 - 2)\ (\alpha_3 - 2)$	2,3,4	2,3,4

Table 13. Lowest four natural frequencies of simple supported epoxy resin square plate.

Mode	m	n	Whitney (1970)	Present method
1st	1	1	245.3945	245.8852
2nd	1	2	613.4863	619.6211
3rd	2	1	613.4863	619.6211
4th	2	2	981.5780	986.3632

square plate. This is because frequency is proportional to $\sqrt{D}$ as seen from Equations 25 and 26, and D is directly proportional to the tensile modulus E. Hence, the frequency increases as E increases. It is seen from Table 3 that the untreated coir fibers reinforced epoxy resin composite plate has higher tensile modulus than other plates; therefore, it has higher frequency values.

- Epoxy resin has less frequency because it has high damping property as compared to other composite plate.

Similarly, as can be observed in case of clamped edge boundary conditions shown in Tables 16–18, there is good agreement in results between Hearmon [30] and present methods. But in clamped boundary conditions, values of frequencies are higher as compared to simple supported boundary conditions.

CONCLUSIONS

The important findings of the present investigation are: Even the tin based halogen compounds act as fire retardant materials. Only 5% (approximate) of fire retardant filler can effectively reduce the smoke density by 25% and increase the LOI value by 24%. The mechanical properties of the finally processed composite materials are not affected much by incorporation of filler, whereas the flexural strength and flexural

Table 14. Lowest four natural frequencies of simple supported treated coir fibers reinforced epoxy resin square composite plate.

Mode	*m*	*n*	Whitney (1970)	Present method
1st	1	1	260.8193	261.3409
2nd	1	2	652.0483	658.5687
3rd	2	1	652.0483	658.5687
4th	2	2	1043.3	1048.4

Table 15. Lowest four natural frequencies of simple supported untreated coir fibers reinforced epoxy resin square composite plate.

Mode	*m*	*n*	Whitney (1970)	Present method
1st	1	1	262.9226	263.4485
2nd	1	2	657.3067	663.8797
3rd	2	1	657.3067	663.8797
4th	2	2	1051.3	1056.8

Table 16. Natural frequencies of the clamped edges epoxy resin square plate.

ω_{mn}	m	n	Hearmon (1959)	Present method
ω_{11}	1	1	449.3277	463.0578
ω_{12}	1	2	916.8079	925.12
ω_{21}	2	1	916.8079	925.12
ω_{22}	2	2	1352.5	1361.5

Table 17. Natural frequencies of clamped edges treated coir fibers reinforced epoxy resin square composite plate.

ω_{mn}	m	n	Hearmon (1959)	Present method
ω_{11}	1	1	477.5712	492.1643
ω_{12}	1	2	974.4358	983.2704
ω_{21}	2	1	974.4358	983.2704
ω_{22}	2	2	1437.50	1447.10

Table 18. Natural frequencies of clamped edges untreated coir fibers reinforced epoxy resin square composite plate.

ω_{mn}	m	n	Hearmon (1959)	Present method
ω_{11}	1	1	481.4226	496.1333
ω_{12}	1	2	982.2942	991.20
ω_{21}	2	1	982.2942	991.20
ω_{22}	2	2	1449.1	1458.8

modulus of the NET increase significantly compared to NEU and NE. The static responses of this composite plate under uniformly distributed can be accurately predicted by multiquadric radial basis function. It is observed that there is a sharp decrease in deflection for aspect ratio, $b/a \leq 2.0$ in both simple supported and clamped edges composite plates and for $b/a \rangle 2.0$ the decrease is gradual.

Further, MQRBF method is used to analyze the dynamic behavior of epoxy resin square plate, untreated coir fiber reinforced composite plate and treated coir fiber reinforced composite plate. Maximum deflection amplitude is highest in epoxy resin square plate and least in untreated coir fiber reinforced composite plate because tensile modulus of the untreated coir fiber reinforced composite plate is higher as compared to treated coir fiber reinforced composite plate and epoxy resin square plate. It means strength of

the untreated coir fiber reinforced composite plate is higher as compared to treated coir fiber reinforced composite plate and epoxy resin square plate. It may be noted here that pure epoxy resin square plate stabilizes fast as compared to untreated coir fiber reinforced composite plate. Actually, after reinforcing the fiber, damping property of the composite plate decreases and stiffness improves. Other reason could be elastic nature of the fiber. When interfacial bonding improves, damping property decreases. Therefore, deflection is less in untreated coir fiber reinforced composite plate and stabilizes slow as compared to pure epoxy resin.

Pure epoxy resin square plate and treated coir fiber reinforced composite plate stabilize at the same time. Coir fibers show lot of porosity under SEM. Since lot of porosity is present on the coir surface, so bromine can easily enter into the pores and react with the inner layer. Diameter of the coir fiber is increased after bromination. Damping property of the treated coir fiber reinforced composite plate increases because coir fibers become brittle due to the treatment from bromine. This improves the stability of the composite plate.

In clamped edge boundary condition, deflection of the plate is less and it stabilizes late as compared to simple supported boundary condition. After comparing the natural frequencies at simple supported and clamped edge boundary conditions following observations are made:

- Values of frequencies are higher in clamped edge boundary conditions as compared to simple supported boundary conditions.
- Values of natural frequencies are higher in untreated coir fibers reinforced epoxy resin square composite plate as compared to treated coir fibers reinforced epoxy resin square composite plate and epoxy resin square plate.

APPENDIX

Multiquadric Method for Governing Differential Equation

Substitution of radial basis function in Equation (20) gives

$$\left(\sum_{j=1}^{N} w_j \frac{\partial^4}{\partial x^4}\varphi_j + 2R^2 \sum_{j=1}^{N} w_j \frac{\partial^4}{\partial x^2 y^2}\varphi_j + \sum_{j=1}^{n} R^4 w_j \frac{\partial^4}{\partial y^4}\varphi_j\right) + \sum_{j=1}^{N} w_j \frac{\partial^2}{\partial t^2}\varphi_j - C_v w_j \frac{\partial}{\partial t}\varphi_j - Q = 0 \tag{27}$$

Substitution of radial basis function in Equation (23)

$$\frac{1}{a^4}\left(\sum_{j=1}^{N} w_j \frac{\partial^4}{\partial x^4}\varphi_j + 2R^2 \sum_{j=1}^{N} w_j \frac{\partial^4}{\partial x^2 y^2}\varphi_j + R^4 \sum_{j=1}^{N} w_j \frac{\partial^4}{\partial y^4}\varphi_j\right) = \lambda^4 \sum_{j=1}^{N} w_j \varphi_j \tag{28}$$

$$\frac{1}{a^4}\left(\frac{\partial^4}{\partial x^4}\varphi_j + 2R^2 \frac{\partial^4}{\partial x^2 y^2}\varphi_j + R^4 \frac{\partial^4}{\partial y^4}\varphi_j\right) \sum_{j=1}^{N} w_j = \lambda^4 \varphi_j \sum_{j=1}^{N} w_j \tag{29}$$

For Simple supported edge

$$x = 0, a \quad \sum_{j=1}^{N} w_j \varphi_j = 0 \tag{30a}$$

$$y = 0, b \quad \sum_{j=1}^{N} w_j \varphi_j = 0 \tag{30b}$$

$$x = 0, a \quad \sum_{j=1}^{N} w_j \frac{\partial^2}{\partial y^2}\varphi_j = 0 \tag{30c}$$

$$y = 0, b \quad \sum_{j=1}^{N} w_j \frac{\partial^2}{\partial y^2}\varphi_j = 0 \tag{30d}$$

For clamped edge

$$x = 0, a \quad \sum_{j=1}^{N} w_j \varphi_j = 0 \tag{31a}$$

$$y = 0, b \quad \sum_{j=1}^{N} w_j \varphi_j = 0 \tag{31b}$$

$$x = 0, a \quad \sum_{j=1}^{N} w_j \frac{\partial}{\partial x}\varphi_j = 0 \tag{31c}$$

$$y = 0, b \quad \sum_{j=1}^{N} w_j \frac{\partial}{\partial y}\varphi_j = 0 \tag{31d}$$

Multiple Regression Analysis

$$Aa = P$$

where A is (l*k) coefficient matrix, a is (k*1) vector, p is (l*1) load vector.

Approximating the solution by introducing the error vector e, we get

$$p = Aa + e$$

Where e is (l*1) vector. To minimize the error norm, let us define a function S as

$$S(a) = e^T e = (p - Aa)^T (p - Aa)$$

The least-square norm must satisfy

$$\left(\frac{\partial S}{\partial a}\right)_a = -2A^T p + 2A^T Aa = 0$$

This can be expressed as

$$a = (A^T A)^{-1} A^T p$$

or

$$a = B.P$$

1. The matrix B is evaluated once and stored for subsequent usages.

NOMENCLATURE

a, b = Dimension of the plates
h = Thickness of the plates
D = Flexural rigidity of plates
ν = Poisson's ratios
w^* = Displacement in z^* direction
w = Dimensionless displacement in z direction
R = Aspect ratio (a/b)
E = Young's modulus

REFERENCES

1. Belystcho, T., Lu, Y. and Gu, L. (1994). Element Free Galerkin Methods, *Int. J. Numer. Meth. Eng.*, **37**: 229–256.
2. Liu, W.K., Jun, S. and Zhang, Y. (1995). Reproducing Kernel Particle Method, *Int. J. Numer. Meth. Eng.*, **20**:1081–10106.
3. Lucy, L.B. (1977). A Numerical Approach to the Testing of the Fission Hypothesis, *Astronom. J.*, **82**(12): 1013–1024.
4. Melenk, J.M. and Babuska, I. (1996). The Partition of Unity Finite Element Method: Basic Theory and Applications, *Comput. Meth. Appl. Mech. Eng.*, **139**: 289–314.
5. Wendland, H. (1995). Piecewise Polynomial Positive, Definite and Compactly Supported Radial Basis Functions of Minimal Degree, *Adv. Comput. Meth.*, **4**: 389–396.
6. Atluri, S.N. and Zhu, T. (1998). A New Meshless Local Petrov–Galerkin (MLPG) Approach in Computational Mechanics. *Comput. Mech.*, **22**: 117–127.
7. Zhang, G.M. and Batra, R.C. (2004). Modified Smoothed Particle Hydrodynamics Method and its Application to Transient Problems, *Comput. Mech.*, **34**(2): 137–146.
8. Duarte, C.A. and Oden, J.T. (1996). H–p Clouds–An hp Meshless Method, Numer. *Meth. Partial. Diff. Equations.*, ▮ 1–34.
9. Nayroles, B., Touzot, G. and Villon, P. (1992). Generalizing the Finite Element Method: Diffuse Approximation and Diffuse Elements, *Comput. Mech.*, **10**: 307–318.
10. Sukumar, N., Moran, B. and Belytschko, T. (1998). The Natural Element Method in Solid Mechanics, *Int. J. Numer. Meth. Eng.*, **43**: 839–887.
11. De, S. and Bathe, K.J. (2000). The Method of Finite Spheres, *Comput. Mech.*, **25**: 329–345.
12. Qian, S. and Weiss, J. (1993). Wavelet and the Numerical Solution of Partial Differential Equations, *J. Comput. Phy.*, **106**: 155–175.
13. Hardy, R.L. (1971). Multiquadric Equations of Topography and Other Irregular Surfaces, *Geophys. Res.*, **176**: 1905–1915.
14. Kansa, E.J. (1990). Multiquadrics—A Scattered Data Approximation Scheme with Applications to Computational Fluid Dynamics, i: Surface Approximations and Partial Derivative Estimates, *Comput. Math. Applic.*, **19**(8/9): 127–145.
15. Fedoseyev, A.I., Friedman, M.J. and Kansa, E.J. (2002). Improved Multiquadric Method for Elliptic Partial Differential Equations via PDE Collocation on the Boundary, *Comput. Math. Applic.*, **43**(3–5): 491–500.
16. Grand, A.F. and Wilkie, C.A. (▮▮▮▮) (eds), *Fire Retardancy of Polymeric Materials*, Marcel Dekker Inc., ▮▮.
17. Rose, N., Le Bras, M., Bourbigot, S., Delobel, R. and Costes, B. (1996). *Polymer Degradation and Stability*, **54**: 355.
18. Nara, S. and Matsuyama, K.J. (1971). *Macromol. Sci. Chem.*, **A5**: 1205.
19. Rose, N., Le Bras, M., Delobel, R., Costes, B. and Henry, Y. (1993). *Polymer. Degradation and Stability.*, **42**: 307.
20. Toldy, A., Anna, P., Marosi, G.Y., Keglevich, G.Y., Almeras, V. and Le Bras, M. (2003). *Polymer. Degradation and Stability.*, **82**: 317.
21. Yang, Y.P., Brewer, D.G. and Venant, J.E.S. (1991). A Study of the Synergistic Action of Antimony Oxide in Fire Retardant Polyethylene, *Fire. Mat.*, **15**(1): 37.
22. Khalturinskii, N.A. and Berlin, A.A. (1990). On Reduction of Combustibility of Polymeric Materials. *Int. J. Polym. Mater.*, **14**: 109.
23. Pillai, M.S. and Vasudev, R. (2001). Application of Coir in Agricultural Textiles, in International Seminar on Technical Textiles, Mumbai, India, June 2–3.
24. Khalid, H.P.S.A., Ismail, H., Rozman, H.D. and Ahmed, M.N. (2001). *Eur. Polym. J.*, **37**: 1037.

25. Ling, L. and Kansa, E.J. (2004). Preconditioning for Radial Basis Functions with Domain Decomposition Methods, *Math. Comput. Modell.*, **40**: 1413–1427.
26. Ferreira, A.J.M., Roque, C.M.C. and Jorge, R.M.N. (2005). Free Vibration Analysis of Symmetric Laminated Composite Plates by FSDT and Radial Basis Functions, *Comput. Meth. Appl. Mech. Eng.*, **194**: 4265–4278.
27. Timoshenko, Stephen. P. and Woinowsky-Krieger, S. (1989). *Theory of Plates and Shells*, McGraw-Hill International Editions, ▮▮▮.
28. Chen, J.T., Chen, I.L., Chen, K.H., Lee, Y.T. and Yeh, Y.T. (2004). A Meshless Method for Free Vibration Analysis of Circular and Rectangular Clamped Plates Using Radial Basis Function. *Engineering Analysis with Boundary Elements*, **28**: 535–545.
29. Ashton, J.E. and Whitney, J.M. (1970). *Theory of Laminated Plates*, Technomic Publishing Co., Inc., ▮▮▮.
30. Hearmon, R.F.S. (1959). The Frequency of Flexural Vibration of Rectangular Orthotropic Plates with Clamped or Supported Edges. Transactions of ASME, *Journal of Applied Mechanics*, ▮▮▮: 537–540.